Charge transfer from Cu in Cu_2O epitaxially grown on MgO(001) by dc-reactive magnetron sputtering

Koji Ogawa, Takahiro Itoh, and Kunisuke Maki*
Graduate School of Integrated Science, Yokohama City University, 22-2 Seto, Kanazawa-ku, Yokohama, Kanagawa 236-0027, Japan
(Received 2 September 1999; revised manuscript received 1 May 2000)

The Cu_2O film is epitaxially grown on air-cleaved MgO(001) by dc-reactive magnetron sputtering. From the reflection high-energy electron diffraction patterns two orientations are identified: (I) $Cu_2O(001)\|MgO(001)$ and $Cu_2O[100]\|MgO[100]$ and (II) $Cu_2O(110)\|MgO(001)$ and $Cu_2O[1\bar{1}0]\|MgO[110]$. The charge transfer Δq^{Cu} from Cu to O is also estimated by Auger electron spectroscopy. Both the Auger intensity ratio O/Cu and Δq^{Cu} increased for the film annealed in O_2, which indicates the as-deposited film is O deficient. From the annealed film Δq^{Cu} for Cu_2O is tentatively taken as $0.65e$ though still O deficient.

Research on epitaxial growth of metal and semiconductor films has a long history, and those of insulator films has also drawn some attention because of their functions such as ferroelectricity and high optical indices of refraction. Since the discovery of superconductivity the attention has become stronger than ever, especially for copper oxides. With these backgrounds our current interest is to clarify the mechanism of epitaxial growth for oxide thin films. Oxides consist of at least two, very often more, elements and these elements form chemical bonds that are mainly ionic. Epitaxial growth of oxide thin films is, therefore, the process that spontaneously adjusts the composition of component elements, the formation of chemical bonds, and the construction of crystal structure. In these terms chemical bonding analysis is necessary in addition to conventional composition and structure analyses for the characterization of films. One way of analyzing chemical bonding states is to determine the degree of ionicity by estimating charge transfer from cations to anions. Previously we showed the formulation how to estimate charge transfer on Cu in oxides by Auger electron spectroscopy-(AES) and reported the result applied to the cleaved surfaces of single crystalline $YBa_2Cu_3O_{7-\delta}$ (YBCO) and $Ba_2Cu_3O_4Cl_2$ (BCOC) (Ref. 1) whose surface structure and composition have less ambiguity than thin films. In this paper, as the next step, we will show the charge transfer in the epitaxial film of Cu_2O. The adopted film preparation method is dc-reactive magnetron sputtering. With this method many authors fabricated not only Cu_2O but also CuO phases mainly by changing O_2 partial pressure.[2–8] These phases were only polycrystalline. To our knowledge, this is the first report of the epitaxial growth of Cu_2O thin film by dc-reactive sputtering. We analyzed the structure by the reflection high-energy electron diffraction (RHEED) technique. We will describe the detail of the structure analysis in a separate paper[9] because of the limited space and concentrate mostly on the composition and chemical bonding analyses in this paper.

We prepared films in a UHV chamber whose base pressure is less than 10^{-8} Torr. The substrate is air-cleaved MgO(001) and the other parameters are listed in Table I. We did not measure the thickness. Since the thickness of metallic Cu film made under the same condition but without O_2 introduction is ~ 1600 Å the thickness of Cu_2O film may be comparable if their deposition rate should be similar.

RHEED patterns are observed in the analyzing chamber connected to the preparation chamber. The samples can be transferred between these two chambers without breaking vacuum. The energy of incident electron is nominally 10 keV and the glancing angle of incidence $\sim 4°$. A goniometer assures the azimuthal rotation of about 100°, which covers from $MgO[1\bar{1}0]$ through [100] to [110]. We confirmed azimuthal angles by observing RHEED patterns from bare regions of MgO substrate. Symmetrical patterns were observed for the incident directions parallel to the [100], $[100]\pm 10°$, and $\langle 110\rangle$ of MgO substrate as shown in Fig. 1. We also showed the predicted patterns based on the Ewald construction method. The predicted patterns are parts of the reciprocal planes intersected by the Ewald sphere. Care was taken to scale them properly. The symbols in the predicted patterns represent the reciprocal lattice points and correspond to the five groups of structure factor S_G (one group of S_G is zero, so only four groups remain). For S_G a usual equation is used: $S_G(hkl)=\Sigma_i f_i \exp[-2\pi i(hkl)\cdot(r_1r_2r_3)]$, where f is the atomic scattering factor, h,k,l are the Miller indices, and $r_{1,2,3}$ the Cartesian coordinates for each ion within the unit cell.[10] Because Cu ions construct a fcc lattice and O ions a bcc lattice in the real lattice, the resulting reciprocal lattice is a mixture of a bcc and a fcc lattices. Since the observed pattern in Fig. 1(a) is indicative of a fcc structure, we assume $Cu_2O(001)\|MgO(001)$ and $Cu_2O[100]\|MgO[100]$ (referred to the orientation I) and predicted patterns as shown also in Fig. 1. A good agreement between the observed and the predicted patterns supports the assumed orientation I. For other two directions, however, the orientation I could not give predicted patterns which agreed with observed ones. So we examined another orientation reported

TABLE I. Preparation conditions.

Parameter	Value
Cathode voltage	-500 V
Cathode current	~ 2 mA
Substrate temperature	~ 710 K
Presputtering time	10 min
Main sputtering time	70 min
O_2 partial pressure	3 mTorr
Total pressure	10 mTorr

 ©2000 The American Physical Society

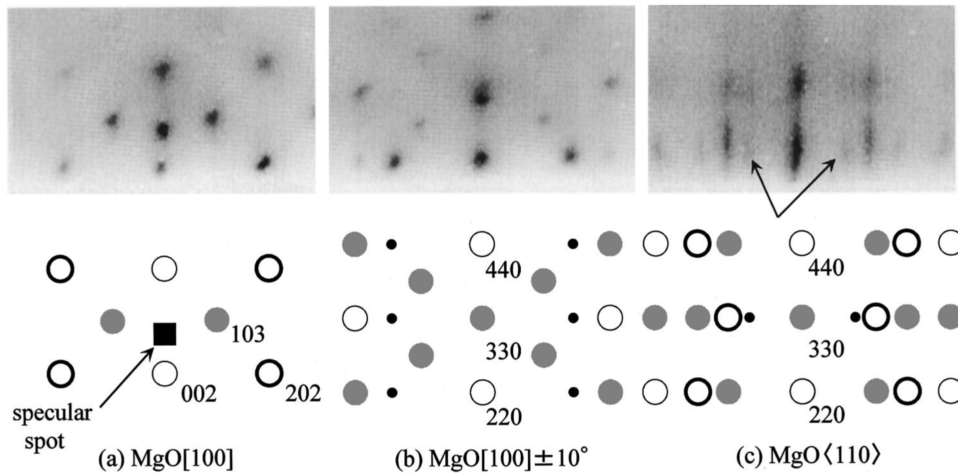

FIG. 1. Observed RHEED patterns and predicted ones based on the Ewald construction for the incident directions parallel to (a) MgO[100], (b) MgO[100]±10°, and (c) MgO⟨110⟩.

by Kawaguchi *et al.* for their molecular-beam-epitaxy-grown Cu_2O films which is $Cu_2O(110)\|MgO(001)$ and $Cu_2O[1\bar{1}0]\|MgO[110]$ (Ref. 11) (referred to the orientation II). The predicted patterns in Figs. 1(b) and 1(c) are based on this orientation II. Agreement between the observed and the predicted patterns is fairly good again for the both incident directions though there are some discrepancy for the MgO⟨110⟩ incidence (the spots in the observed pattern indicated by arrows have no corresponding ones in the predicted pattern). We thus concluded two orientations: (I) $Cu_2O(001)\|MgO(001)$ and $Cu_2O[100]\|MgO[100]$ and (II) $Cu_2O(110)\|MgO(001)$ and $Cu_2O[1\bar{1}0]\|MgO[110]$.

The lattice mismatch for the orientation I is only 1.4% [a_{Cu_2O} is 4.27 Å and a_{MgO} 4.21 Å (Ref. 12)] and is smaller than for the orientation II (−4.4% for $Cu_2O[001]$). Electrostatic matching is better for the former, too. In other words, Cu and O ions can be placed on top of O and Mg ions in the substrate, respectively. However $Cu_2O(001)$ plane consists of O (or Cu) ions alone and is polar. $Cu_2O(110)$ plane, on the other hand, is composed of both ions and is almost nonpolar. These results indicate that surface polarity influences on film orientation as much as the former two factors. We are currently undertaking the film preparation with different sputtering times in order to elucidate the dependency of orientation on thickness. Our preliminary results indicate that the RHEED patterns from films of 30-min or less sputtering times shows $Cu_2O(110)$ and new orientation other than $Cu_2O(001)$, O_2 partial pressure ranging from 2 to 5 mTorr. We assigned this orientation as $Cu_2O(111)$ from their spot and/or streak separation and symmetry. The degree of electrostatic matching may be similar for $Cu_2O(001)$ and (111) orientations. Since lattice mismatch is bigger for $Cu_2O(111)$ (−12.2% for $Cu_2O\langle 11\bar{2}\rangle$) than for $Cu_2O(001)$ orientation, we speculate that the degree of surface polarity may significantly differ and overcome the difference in lattice mismatch. Before concluding the dependency of orientation on thickness we will prepare more films and examine detailed tendency by changing both of sputtering time and oxygen partial pressure systematically. We will report the results also in a forthcoming paper.[9]

We conducted AES measurements with an Auger microprobe (JAMP10S, JEOL) equipped also in the analyzing chamber. The electron beam is incident at the angle of 40° from the surface normal with nominal acceleration voltage of 3 kV. The current is 2.0×10^{-7} A. The detail of the chemical bonding analysis was described in the previous paper[1] and we briefly explain the main points avoiding the repetition of the full story. We first assume that Auger transition intensity is proportional to the charges of the levels involved in the transition as Weißmann did.[13] We took notice of the L_3MM transitions for Cu since these transitions give relatively strong intensities. By measuring the intensities of three main transitions, namely, $L_3M_{23}M_{23}$, $L_3M_{23}M_{45}$, and $L_3M_{45}M_{45}$ transitions, we can gain information on its charge. We denote the charge of M_{45} level as $(N-\Delta q^{Cu})e$, where N is the number of valence electrons, Δq^{Cu} charge transfer from Cu, and e the elementary electric charge. We next introduce another parameter, the Auger transition probability $\omega^{Cu}_{L_3MM}$, which is directly calculated from the intensi-

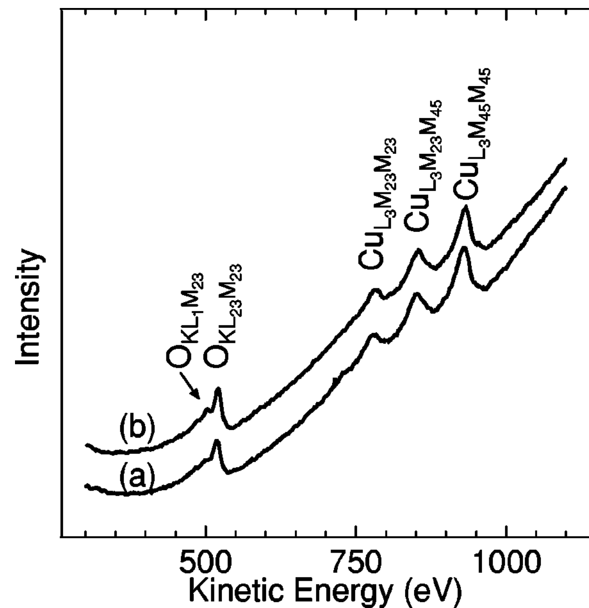

FIG. 2. AES spectra for the as-deposited film (a) and the annealed film (b).

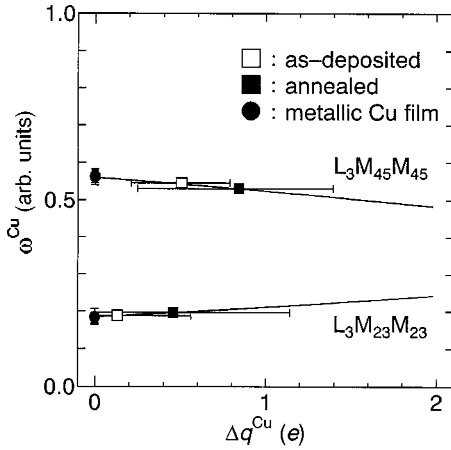

FIG. 3. Relationship between $\omega^{Cu}_{L_3MM}$ and Δq^{Cu}. $\omega^{Cu}_{L_3MM}$ for the metallic film, the as-deposited, and the annealed films are plotted.

ties. In practice, we utilize not intensities but intensity ratios because intensities contain contribution from many factors such as ionization cross section that are difficult to evaluate with sufficient accuracy. We can get the semiempirical relationship between $\omega^{Cu}_{L_3MM}$ and Δq^{Cu} from the intensities measured for the standard sample which is metallic Cu film ($\Delta q^{Cu} \equiv 0.0e$). We can finally determine Δq^{Cu} for copper oxides by plotting $\omega^{Cu}_{L_3MM}$ for them on the semiempirical curves.

Figure 2(a) shows one of the AES spectra for the as-deposited film. We define the intensity as high-energy halves of peak-to-peak height for the differentiated spectra because energy-loss peaks due to inelastic scattering may deform low-energy halves. We repeated measurements on many sites of the film and employed the mean value as the intensities. The experimental errors are their standard deviation. The result for the film is shown in Fig. 3 whose values are listed in Table II. Δq^{Cu} for the $L_3M_{23}M_{23}$ transition is smaller than Δq^{Cu} for the $L_3M_{45}M_{45}$ transition as is the case with YBCO and BCOC.[1] We still have no clear explanation and tentatively took the average. The average operation is supported by the result for YBCO where the agreement with other reports by x-ray photoelectron became better.[1] So Δq^{Cu} is $0.34e$.

Δq^{Cu} is supposed to be unity for the perfect structure and stoichiometry and the purely ionic chemical bonding. However, Δq^{Cu} for the as-deposited film is much smaller. We then speculated that oxygen might be deficient. In order to examine the speculation we annealed the as-deposited film in the O_2 atmosphere, though interpretation of the annealing effect might be difficult because the recovery of O deficiency is a rather complicated process that involves diffusion and/or dissociation of O_2 and chemical reaction with Cu. The annealing time was 10 min at ~ 710 K in the O_2 atmosphere of $p_{O_2} = 4$ mTorr. The heating and cooling procedures are the same as the one for preparation. The annealing made a noticeable change in the RHEED pattern only for the MgO⟨110⟩ incidence. New streaks appeared between the (00) and adjacent streaks in Fig. 1(c). Upon annealing the Auger intensity ratio O/Cu increased by $\sim 30\%$ from 1.4 ± 0.14 to 1.8 ± 0.19, where the evaluated transitions are the $KL_{23}L_{23}$ and the $L_3M_{45}M_{45}$ transitions for O and Cu, respectively. Care was taken to make measurements on the same region of the film before and after annealing. One of the AES spectra for the annealed film is shown in Fig. 2(b). The increase in the ratio O/Cu supports our assumption. So we concluded that the as-deposited film was O deficient and supposed that the enlargement of the error bars might be due to the nonuniformity of the annealing effect. Δq^{Cu} almost doubled to be 0.65, which was also averaged for the $L_3M_{45}M_{45}$ and the $L_3M_{23}M_{23}$ transitions (see Table II). Though the annealed film may still be O deficient we tentatively took Δq^{Cu} for Cu_2O as $0.65e$. In order to judge if this value is reasonable we refer to the literature. Since we could not find experimental values for Cu in Cu_2O such as the effective charge determined from the angular frequencies for phonon excitation we cite the theoretical values only. The values are briefly reviewed by Ruiz *et al.* and are shown to be controversial.[14] The values range from 0.43 to $0.97e$.[14–18] The best agreed value is $0.65e$ by Goodman *et al.* using the Hartree-Fock-Slater method.[17] Our result supports the calculation by Goodman *et al.*; however, more comparisons would be required to prove the correspondence.

TABLE II. Values of $\omega^{Cu}_{L_3MM}$ calculated from measured intensities and of the determined $\Delta q^{Cu}_{L_3MM}$.

	Transition	ω^{Cu}	Δq^{Cu}
As-deposited	$L_3M_{23}M_{23}$	0.188	$0.13^{+0.43}_{-0.13}$
film	$L_3M_{45}M_{45}$	0.543	$0.54^{+0.28}_{-0.29}$
Annealed	$L_3M_{23}M_{23}$	0.196	$0.46^{+0.68}_{-0.46}$
film	$L_3M_{45}M_{45}$	0.530	$0.84^{+0.55}_{-0.60}$

It is not straightforward to reasonably interpret the correspondence between the increases in the ratio O/Cu by $\sim 30\%$ and in Δq^{Cu} by $\sim 90\%$. We may suppose a nonuniform effect of the O_2 anneal in the direction normal to the surface. That is, O_2 or dissociated O may diffuse more readily in the structure with O deficiency than in more stoichiometric region. Diffusing inward more and more, O will accumulate at a relatively deep region after some recovery of the O deficiency there. O enrichment may, hence, become greater in the relatively deep region than in the surface region. A second possibility is the following. After the preparation of films we observe RHEED patterns first in order to determine measurement areas for AES. During the observation the films may become O deficient just as some oxides that are known to be unstable at room temperature[19] and/or to electron irradiation[20,21] and thus prone to O deficiency. O_{KLL} Auger electrons from the region may attenuate severely. Cu_{L_3MM} Auger electrons may attenuate as well, but the degree of attenuation may be similar among the $L_3M_{23}M_{23}$, $L_3M_{23}M_{45}$, and $L_3M_{45}M_{45}$ transitions because the kinetic energies are close. Since calculated not from the intensities but from the intensity ratios of Cu_{L_3MM} Auger electrons $\omega^{Cu}_{L_3MM}$ and also Δq^{Cu} would be insensitive to the attenuation and reflect the contribution from the deep, O-enriched, hence possibly more ionic region. The above argument does not contradict with the RHEED observations since RHEED patterns reflect only the surface region due to the grazing incidence.

In summary, we grew the epitaxial film of Cu_2O by dc-reactive magnetron sputtering. From the comparison between the predicted based on the Ewald construction and the observed RHEED patterns we identified two epitaxial orientations: (I) $Cu_2O(001)\|MgO(001)$ and $Cu_2O[100]\|MgO[100]$ and (II) $Cu_2O(110)\|MgO(001)$ and $Cu_2O[1\bar{1}0]\|MgO[110]$. By AES on the as-deposited and the O_2 annealed films we concluded that the as-deposited film was O deficient. From the result on the annealed film we tentatively took Δq^{Cu} for Cu_2O as $0.65e$ though the annealed may still be O deficient.

We are grateful to Center for Industrial Technology & Design, Yokohama City for atomic-force microscopy measurements.

*Author to whom correspondence should be addressed. Electronic address: sfsmaki@yokohama-cu.ac.jp

[1] K. Ogawa, S. Noro, and K. Maki, J. Appl. Phys. **82**, 1640 (1997).
[2] V.F. Drobny and D.L. Pulfrey, Thin Solid Films **61**, 89 (1979).
[3] G. Beensh-Marchwicka, L. Kròl-Stępniewska, and M. Słaby, Thin Solid Films **88**, 33 (1980).
[4] W. Klein, H. Schmitt, and M. Böffgen, Thin Solid Films **191**, 247 (1990).
[5] G.M. Rao *et al.*, Thin Solid Films **207**, 29 (1992).
[6] A. Parretta *et al.*, Phys. Status Solidi A **155**, 399 (1996).
[7] K. Wasa and S. Hayakawa, *Handbook of Sputter Deposition Technology* (Noyes, Park Ridge, NJ, 1992).
[8] T. Fujii, M. Takano, R. Katano, and Y. Bando, J. Appl. Phys. **66**, 3168 (1989).
[9] K. Ogawa, T. Itoh, and K. Maki (unpublished).
[10] C. Kittel, *Introduction to Solid State Physics*, 6th ed. (Wiley, New York, 1986).
[11] K. Kawaguchi, R. Kita, M. Nishiyama, and T. Morishita, J. Cryst. Growth **143**, 221 (1994).
[12] R. W. G. Wyckoff, *Crystal Structures*, 2nd ed. (Wiley, New York, 1963), Vol. 1.
[13] R. Weißmann, Solid State Commun. **31**, 347 (1979); R. Weißmann and K. Mueller, Surf. Sci. Rep. **1**, 251 (1981).
[14] E. Ruiz, S. Alvarez, P. Alemany, and R.A. Evarestov, Phys. Rev. B **56**, 7189 (1997).
[15] W.Y. Ching, Y.-N. Xu, and K.W. Wong, Phys. Rev. B **40**, 7684 (1989).
[16] S. Nagel, J. Phys. Chem. Solids **46**, 743 (1985).
[17] G.L. Goodman, D.E. Ellis, E.E. Alp, and L. Soderholm, J. Chem. Phys. **91**, 2983 (1989).
[18] R.A. Evarestov and V.A. Veryazov, Phys. Status Solidi B **157**, 281 (1990).
[19] A.J. Arko *et al.*, Phys. Rev. B **40**, 2268 (1989).
[20] S. Ichimura and R. Shimizu, J. Appl. Phys. **50**, 6020 (1979).
[21] P.J. Feibelman and M.L. Knotek, Phys. Rev. B **18**, 6531 (1978).